Review on hydrogen leak detection: comparison between fiber optic sensors based on different designs with palladium

Nicolas Javahiraly

Review on hydrogen leak detection: comparison between fiber optic sensors based on different designs with palladium

Nicolas Javahiraly*
University of Strasbourg, ICube Institute, 300 Boulevard Sébastien Brant CS10413, 67412 Illkirch cédex, France

Abstract. A review of optical fiber hydrogen sensors based on palladium (Pd) is presented. Palladium hydrogen optical fiber sensing systems can be considered as a model for other metal hybrid systems. In addition, the Pd hydrogen systems are well characterized in bulk, cluster, or thin film form. We focus on the fiber principles. We then discuss their performances regarding their configurations. We will conclude by introducing the challenges in designing an ideal hydrogen optical fiber sensor based on a metal hybrids approach and which design direction is considered the best to take. © *2015 Society of Photo-Optical Instrumentation Engineers (SPIE)* [DOI: 10.1117/1.OE.54.3.030901]

1 Introduction

We present a review of optical fiber hydrogen sensors based on palladium (Pd). Palladium hydrogen optical fiber sensing systems can be considered as a model for other metal hybrid systems. In addition, the Pd hydrogen systems are well characterized in bulk, cluster, or thin film form. We focus on the fiber principles. The first part describes the phase-, polarization-, intensity-, and wavelength-modulated hydrogen sensors responses of existing sensors. In the second part, we discuss their performances regarding their configurations. We will conclude by introducing the challenges in designing an ideal hydrogen optical fiber sensor (OFS).

2 Optical Fiber Hydrogen Sensors Based on Palladium Principles

2.1 Typical Hydrogen Sensor Response Based on Palladium

Hydrogen sensors based on Pd measure the physical changes in Pd during the hydrogenation. From the Pd physical changes, which are related to the hydrogen solubility, we can have access to the hydrogen concentration in the surrounding environment. Thus, the sensor responses typically show the same aspects as the pressure-composition-isotherm curves.

At room temperature,

- for a hydrogen concentration corresponding to the α phase, the signal changes slightly due to the low hydrogen solubility in the metal;
- at the phase transition, a large change is observed corresponding to a large increase of the hydrogen amount in the metal; and

- for a hydrogen concentration corresponding to the β phase, the signal saturates since the Pd hydride film is completely hydrogenated.

For optical sensors, the measured changes are the Pd dielectric permittivity and/or the Pd lattice constant. The challenge in designing an OFS for hydrogen leak detection is to make the optical fiber sensitive to the α-phase when small changes occur. Furthermore, the dynamic range is an issue when hydrogen quantification is required. Note that the hysteresis is not an issue in our case, but it is important when the quantitative monitoring of hydrogen concentrations is required.
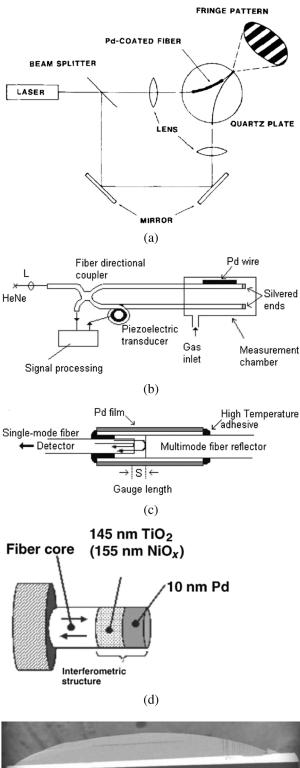
2.2 Phase-Modulated Hydrogen Sensor Responses

Figure 1 presents several interferometers for hydrogen detection.

2.2.1 Butler's interferometer

Butler[2,3] developed the first OFS for hydrogen detection in 1984. The device consists of a Mach–Zehnder fiber interferometer [Fig. 1(a)]. It combines two single-mode optical fibers (ITT-1601) with optical elements to achieve the interferometer. The light of a He-Ne laser, 0.5 mW, is split by a beam splitter and injected into both optical fibers by lenses. One is sensitive to hydrogen, whereas the second is insensitive. The jacket is mechanically removed for both fibers over a length of 3 cm. A Pd layer of 10-μm thickness is sputtered in Ar with an initial 10-nm thick Ti (Titanium) layer (providing a good adhesion between the metal and the optical fiber) on the first unjacketed fiber, whereas a Pt (Platinum) layer is deposited on the second one in order to maintain, if possible, the same temperature dependence between both fibers. Both optical fibers are glued to a fused quartz plate to rigidify the structure. The expansion of the Pd upon hydrogenation results in stretching one fiber in both axial and radial directions and changing its effective path length. The change in optical path length results in a fringe pattern at the output of the interferometer, visually observable and recordable with a

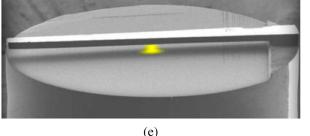*Address all correspondence to: Nicolas Javahiraly, E-mail: n.javahiraly@unistra.fr

(a)

(b)

(c)

(d)

(e)

Fig. 1 Interferometer design for hydrogen sensor: (a) Mach–Zehnder, (b) Michelson, (c) and (d) Fabry–Perot (FP) fiber and a FP interferometer sensor developed by Maciak et al.,[1] and (e) fiber tip cantilever.

simple photodetector. The shift of the fringe is then related to the hydrogen concentration. The signal resolution is limited by the noise which comes from the sensitivity of the sensor to vibrations and sound.

The hydrogenation was carried out with different carrier gases (Ar, N_2, and dry air) showing different response times. They observed that the response time, in the order of a few minutes, was longer than the diffusion constant for hydrogen in Pd. From these observations, they suggested that the kinetics is dominated by the surface reactions at room temperature.

Finally, they estimated a range from $10^{-4}\%$ (1 ppm) to 3% H_2 for the sensitivity. The lower limit is determined by temperature fluctuation. The upper limit corresponds to the β-phase, because they considered only the regime of the α-phase in order to relate the hydrogen partial pressure to the hydride composition (Sieverts equation). In 1988, they reported a response in a range from $2\times10^{-6}\%$ (20 ppb) to 3% H_2 for different film thicknesses deposited by sputter and electrodeposition[3] [Fig. 1(a)].

For a concentration above 0.1% H_2, the experimental result follows the Sieverts law, explained by the linear relationship between the lattice constant and hydrogen content.[4] At lower concentrations, a large deviation is observed. The observed fringe shift, which is larger than expected from even the enhanced Sievert component, suggests an additional trappings site for hydrogen with a binding energy larger than the anomalous bulk behavior [Fig. 2]. The authors assumed that the fringe shift observed is likely due to the binding at a free metal surface.

Theoretically, the optical path length in the fiber core is related to the strain in the fiber core by the elasto-optic equation:[5]

$$\frac{\Delta\varnothing}{\varnothing} = e_z - \frac{n^2}{2}[2e_r(p_{11} - p_{44}) + e_z(p_{11} - 2p_{22})],$$

where n is the index of refraction of the fiber, p_{ij} are the Pockels coefficients, and e_z and e_r are the axial and radial strains in the fiber core. Butler et al. theoretically studied the sensor response by solving the stress-strain relationships for this structure with the appropriate boundary conditions. They considered a one-dimensional model which only takes into account the axial strain (and assumes a given value for the radial strain).

2.2.2 *Interferometer Development*

Faralhi et al.[6] demonstrated the feasibility of an all single-mode optical fiber Michelson interferometer for H_2 sensing [Fig. 1(b)]. (A Michelson interferometer is a Mach–Zehnder interferometer that has been folded back upon itself.) A He-Ne laser, 0.2 mW, is split into two single-mode fibers (SMFs) and recombined by a fiber direction coupler (FC). The measurement is based on a pseudoheterodyne scheme[7] to eliminate the differential drift in the arms of the SMF interferometer. A part of the reference fiber is wound onto a driven piezoelectric cylinder. The signal is, therefore, modulated at a frequency of the applied voltage. On the sensing fiber, a Pd wire, with a length and diameter, respectively, of 6 cm and 500 μm, is attached on the optical fiber (without the jacket) using quick-setting epoxy resin.

As for Butler's sensor, the Pd expansion upon hydrogenation causes a change of the fiber sensing length, which results in a phase retardance. The thermally induced effect of the hydrogenation (exothermic reaction) is small compared with the axial strain when the reaction takes place at room temperature and at a low concentration (α-phase). The sensor responses to a range of 0.0054% (54 ppm) to 1.5% H_2 in N_2 at 1 atm, with a response time of a few minutes. The resolution is 2 Pa limited by the differential thermal fluctuations.

In order to avoid polarization problems and to detect a single axial strain, in 1994, Zeakes et al.[8] developed an extrinsic Fabry–Perot (FP) interferometric sensor [Fig. 1(c)]. The device consists of putting a multimode fiber (MMF) at a distance S from an SMF in a glass alignment tube to achieve a FP cavity. A 2-μm layer of Pd is sputtered on this tube.

Upon hydrogenation, the Pd expansion changes the length of the cavity S. The output intensity is described by

$$I = I_0 \left[1 + \cos\ 1 + \frac{4\pi S}{\lambda} \right],$$

where $\lambda = 1300$ nm is the source wavelength. As a result, the intensity of the light is modulated as a function of hydrogen concentration. The sensor response was verified at 0.5% and 5% H_2 in N_2 showing the fringe shift with a response time faster than a minute. The response is not reproducible over hydrogenation cycles due to the delamination of the Pd film.

The hydrogen interferometer sensors based on the Pd expansion presented here use thick films. Pd thick films show a poor reproducibility over ab-desorption cycles. After a few cycles, irreversible microcracks appear. Moreover, the observed response time is too slow due to the diffusion limitation. Therefore, this technology has been put aside during a decade. Recently, interferometers have received renewed attention due to their high sensitivity potential. New designs based on thin films have been studied.

Innnuzzi et al.[9] proposed a hydrogen fiber top cantilever sensor. The sensor consisted of achieving an FP cavity between the fiber tip and the cantilever [Fig. 1(e)]. The light scattered back into the fiber encounters an optical FC, which couples 50% of the reflected beam into another fiber that is aligned with an infrared photodiode. A 150-nm Pd film with a 10-nm chromium substrate layer is deposited on the cantilever. The output of the photodiode W, as for Zeakes's sensor, is given by

$$W = W_0 \left[1 - V \cos\left(\frac{4\pi d}{\lambda} \right) \right],$$

where d is the distance between the fiber-to-air and the air-to-cantilever interfaces, V is the fringe visibility relative to the interference of the three reflected signals, and W_0 is the midpoint output. Due to the Pd expansion in the presence of hydrogen the cantilever bends, which results in the cavity length change. The sensor responds to 4% H_2 in Ar. However, the performances of the device are seriously damaged over ab-desorption hydrogen cycles.

Maciak et al. developed a simple optical FP fiber interferometer. It consisted of a deposited layered sensing structure made of 145-nm TiO_2 and 10-nm Pd at the tip of fiber, as depicted in Fig. 1(e). The first mirror is achieved on the
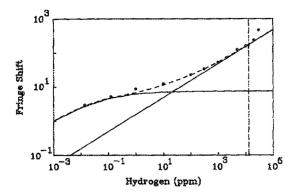

Fig. 2 The fringe shift for a fiber sensor as a function of hydrogen concentration. The vertical dashed line indicates the upper edge of the α-phase boundary. The straight solid line is the Sieverts law component of the response, and the curved line is the response from the deeply bound sites (these sites correspond likely to binding at a free-metal surface) described by a Langmuir isotherm. The dashed line is the sum of these two contributions.[3]

fiber/TiO_2 boundary, whereas the Pd layer plays the role of the second mirror and promotes the dissociation of hydrogen. The TiO_2 layer is the resonance cavity of the interferometer and the sensitive layer. According to the authors, the contribution of the Pd layer to the optical signal is minimum.

The sensor responds from 1% to 3.5% H_2 in synthetic air with a response time that is faster than 1 min. The response is reproducible. A large change is obtained at 2% after which the signal response is saturated.

We conclude from the hydrogen response that the sensor response is likely due to the hydrogenation of the Pd layer.

Lately, Kim et al.[10] proposed a Mach–Zehnder fiber optic interferometer achieved by two identical long-period gratings (LPGs); each had a 500-μm period and was characterized by a length of 20 mm and a center-to-center distance of 50 mm. A 50-nm thick Pd film was uniformly deposited over the cladding of an SMF. This sensor is sensitive to the change of the refractive index of the Pd. During Pd hydrogenation, the effective index of the cavity changes, which result in the changing of the effective optical path length. The response sensor was only measured at a concentration of 4% H_2 in N_2. The response time is approximately 8 min.

2.3 Polarization-Modulated Hydrogen Sensor Responses

In continuation of Butler's interferometric fiber sensors, in 1992, Dessy and Richmond[11] developed a hydrogen sensor based on polarization modulation by using a Pd thin film. In this case, the sensor did not use the Pd expansion, but instead used the heat released from the chemical reaction. The device consisted of a single-mode birefringence fiber maintained in a metal sheath. The cladding was removed on a part of the fiber and replaced by a 6-nm Pd layer.

The change in temperature during the reaction causes a change in the birefringence of the optical fiber. Orthogonal modes HE_{11x} and HE_{11y} (fundamental modes) both propagate through the fiber with different propagation constants. Due to the coupling between both modes, the polarization is changed. The strain induced by the Pd expansion is neglected; the sensor acts as a thermal sensor. The sensor detects a concentration range from 1% to 10% H_2 in inert

gas. The loading time is about 1 min at a concentration of 2.8%.

2.4 Intensity-Modulated Hydrogen Sensor Responses

2.4.1 Micromirror sensors

Micromirror sensors[12–15] probably constitute the most mature and simple hydrogen sensing devices. A Pd thin film is deposited on one cleaved end of a multimode optical fiber. The other end of the optical fiber is connected to a Y coupler, which allows the illumination of the sensing film and the collection of the reflected light from the latter [Fig. 3(a)].

The reflectance R (and transmittance T) of the Pd film changes as a function of H_2 uptake due to a decrease of the Pd hydride refractive index. By measuring the reflected intensity, the optical change is related to hydrogen concentration.

In 1991, Butler et al. described the response of a 10-nm Pd film deposited on an MMF end with a 125-μm diameter. Figure 3(b) shows the reflected light for different hydrogen concentrations. The reflectance changes continuously depending on the hydrogen concentration.[13,16] In particular, they have observed that the reflectivity change is a measure of the composition of the Pd hydride. The plot of the relative change in reflectivity as a semilog function of H_2 concentration shows the pressure composition isotherms (pcts) of Pd for different temperatures [Fig. 3(c)]. The slope of the plateau region observed is characteristic of thin films.

The sensor response is reproducible over hydrogen cycles, but different responses are obtained for identical sensors. The authors suggested that this difference comes from an uncontrollable parameter during the deposition process. They observed, in fact, two trends for the change in the relative reflectivity independent of the thickness of the film (10 to 70 nm). While some thin films exhibit reversible microblistering and microcracking, some films, such as thicker films (100-nm PD[17]) show permanent mechanical failure of film. The microblistering and microcracking are eliminated by depositing a 1- to 2-nm thick Ni (Nickel) underlayer as an adhesive agent, improving the sensor reproducibility. In addition, the change in reflectivity for the Ni/Pd film upon hydrogenation is reduced compared with the Pd film. The level and the width of the plateau region are different as depicted in Fig. 3(d) (circle symbol and line for the Pd/Ni and Pd film, respectively). The authors suggested that this difference is due to the clamping effect of the Pd on the substrate (quartz or Ni). Reversible microblistering, so-called buckles, and the clamping effect have now been well investigated and proven to be related to the stress relaxation.[18]

2.4.2 Micromirror development

In continuation of Butler's work, in 1998, Bevenot[16] described the response of a 13-nm Pd deposited on an MMF, 400-μm-core diameter, in a wide range of temperatures: between −196°C and 23°C. As previously noted, the response change depends on the temperature and is explicitly related to the isotherm pressure equilibrium. A larger signal change is obtained at lower temperatures since the level of the pressure plateau decreases and its width increases. On the other hand, the response time is slower at low temperatures. A response time of 14 s and 100 min, respectively, is
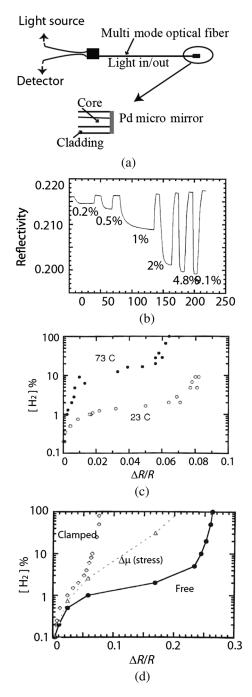

(a)

(b)

(c)

(d)

Fig. 3 (a) Schematic of optical fiber hydrogen sensor based on a micromirror; (b) response of the Butler's micromirror sensor to different [H_2] from Ref. 12; (c) and (d) hydrogen concentration versus reflectivity change for 10-nm Pd film at (c) two different temperatures and (d) for clamped and unclamped films. The dashed line represents the theoretical stress in the clamped film (from Ref. 13).

obtained at 23°C and −45°C for 4% H_2 in N_2. To improve the temperature range of the sensor, they proposed to heat the sample with a power laser diode in order to enhance the response time.

Kazemi et al. developed a micromirror based on colorimetric material.[19] The colorimetric material consisted of inserted Pd into a porous substrate. This micromirror sensor showed a very good reproducibility and reliability. They proved the reliability of the sensor by performing the test

of an Evolved Expendable Launch Vehicle (EELV)/Delta IV engine stand at NASA's Stennis Space Center.

2.4.3 *Characterization of Pd thin film*

In addition to the micromirror results, several studies have been reported to characterize the hydrogenation of Pd thin film deposited on a flat substrate. These studies emphasized the relation between the optical change and the pct. As these studies are based on flat substrate, they provide a simple tool to investigate the properties of Pd thin film and consequently optimize the performances of hydrogen sensors based on Pd.

In 1996, Garcia and Mandelis studied the transmittance of Pd thin film. The film deposited on a glass substrate is illuminated by an optical fiber, and a second fiber collects the transmitted light through the sample. As for the reflectance measurement, the graph of the optical transmittance as a function of hydrogen concentration on a logarithm axis [Fig. 4(a)] shows the equilibrium isotherm pressure curves,[20] in agreement with the literature.

Later, Kalli et al.[21] studied the reflectivity of a Pd film varying from a thickness of 1 to 30 nm and characterized the α- and β-phase transitions after both single and multiple gas cycles from the reflectivity measurement. In particular, they demonstrated that the change of reflectivity depends on the Pd thickness and on the substrate.

Figures 4(b) and 4(c) show the reflectivity for 1- and 3-nm thick Pd film, respectively, upon hydrogen exposure. Remarkably, the reflectivity increases upon hydrogenation for a thickness inferior to 3 nm, whereas the reflectivity decreases upon hydrogenation for a thicker film as previously described. Figure 4(d) shows the influence of the used substrate on the hydrogen response. A higher change is obtained for SiO_2 as a substrate. Moreover, they observed that the structural changes of the Pd film on the silicon nitride, induced via exposure to hydrogen due to surface energy effects, resulted in the creation of nanostructures.

Lately, Matelon et al.[22] showed that the response time is also strongly dependent on the different substrates used. Maximum values of 700 s for Pd/Si and 3700 s for Pd/Al_2O_3 were, for instance, recorded at pressures corresponding to Pd hydride α- to β-phase transition. They attributed this difference to the substrate roughness which modifies the Pd subsurface microstructure.

Recently, the optical transmittance study of metal/metal hydride thin film allows investigating and identifying new hydrogen storage materials.[23,24]

2.4.4 *Evanescent wave hydrogen sensor responses*

The principle is presented in Fig. 5.

In 1999, Tabib-Azar et al.[25] described an optical fiber hydrogen sensor which takes advantage of the evanescent fields associated with the guided light. The device consisted of removing the optical cladding of an MMF (50 μm) and replacing it by a 10-nm Pd film, with an interaction length of 1.5 cm. The optical fiber is illuminated with a light source with a wavelength of 650 nm. In the presence of hydrogen (between 0.2% and 0.6% H_2 in N_2), the transmitted intensity increases with a response time of about 30 s [Fig. 6(a)]. The intensity change is a function of hydrogen concentration [Fig. 6(b)]. According to the authors, the increase in intensity is explained by the decrease of the imaginary part of the Pd
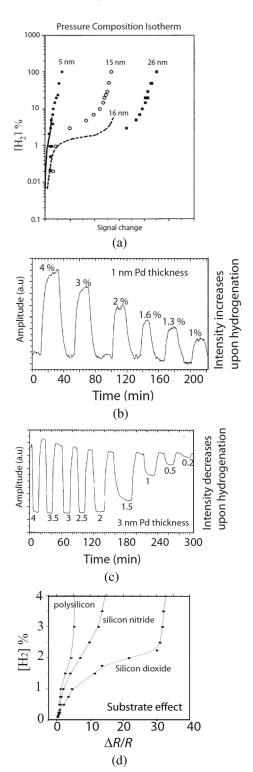

(a)

(b)

(c)

(d)

Fig. 4 (a) Measured isotherm by transmittance for Pd at 25 deg, from Ref. 20, reported by J.A. Garcia et al.; (b) reflectivity change as a function of [H_2] for 1- and 3-nm Pd films; (c-d) relative change of the reflectivity versus [H_2] for different substrates.

refractive index upon hydrogenation. In fact, the transmitted light is less attenuated through the Pd hydride section, since the Pd hydride is less absorbing than Pd. In addition, the authors claimed that the change in the real part of the Pd refractive index results in an effective phase change in the guided light.
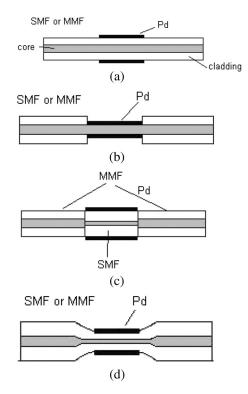
Fig. 5 Schematic of the optical fiber hydrogen sensor based on evanescent field. Pd coated on the (a) cladding, (b) core, and (d) tapered core of MMF (multimode fiber) or SMF (single-mode fiber). (c) Pd coated on heterostructure.

In this case, the situation is, in fact, slightly different. Since the optical cladding is removed and replaced by a Pd film, the Pd layer plays now the role of the optical cladding. Therefore, a new numerical aperture (NA) is defined for the sensing section. Upon hydrogenation, the change of the real part of the refractive index also results in a change of the transmitted intensity since the NA of the sensing section will be modified.

Evanescent wave (EW) sensors are based on the alteration of the evanescent field of the propagating mode. In the general case of optical fiber (multimode, single-mode, tapered fiber, and so on), the transmission intensity I_t of a fiber, when exposed to hydrogen, can be expressed by[26]

$$I_t = I_0 \exp(-2r\Delta\alpha L).$$

I_0 is the transmitted optical power without hydrogen, and r is the ratio of the power of the EWs on the total power of the guided light. r depends on the configuration: r is inferior to 1%, about 1%, inferior to 20%, superior to 50%, and can reach 100% for, respectively, a multimode, a heterostructure, a tapered MMF, an SMF, and a nanofiber. L is the interaction length and α is the variation of absorption between the absorption coefficient of the Pd hydride and the Pd film. The sensitivity of the sensor is tuned by both parameters r and L. The sensitivity of the sensor is enhanced when their values increase.

EW development: Villatoro et al. reported the response of a Pd-coated mulitmode tapered fiber (MMTF[26]), a nanotapered fiber[27] and a single-mode tapered fiber (SMTF[28,29]).

For SMTF,[28] a 12-nm Pd layer with a length of 1.5 cm was deposited on the tapered fiber. The transmitted intensity

increased upon Pd hydrogenation since $\Delta\alpha < 0$. The intensity change was hydrogen dependent [Fig. 6(d)] in a range from 1.8% to 10% H_2 in Ar. In addition, the sensor was polarization independent: the same response for TE (transverse electric) and TM (transverse magnetic) polarizations was obtained. The sensor was also wavelength dependent: a large intensity change is observed for the longer wavelengths in the spectral range of 900 to 1600 nm [Fig. 6(a)].

Although MMTF showed a lower sensitivity than SMTF, it was proposed by Villatoro et al. as a more robust and convenient sensor. The sensor consisted of depositing a 15-nm Pd layer on the taper waist over a length of 1 cm.[26] The waist was in the range of 30 to 70 μm. Two Pd layers were deposited over the taper on the uniform section, with one layer every 180 deg. The measurements were carried out with an LED at a wavelength of 850 nm with an optical power of 20 μm.

The transmitted intensity increased upon Pd hydrogenation ($\Delta\alpha < 0$) [Fig. 6(e)]. They detected hydrogen concentrations ranging from 0.3% to 3.5% H_2. The minimal value was limited by the intensity noise present in the signal. Above 3.5% H_2, the signal was saturated for all the taper waist sensors considered. Nevertheless, the sensor performance can be adjusted with the taper diameter [Fig. 6(f)] in the detected range. The maximal change was found for a thinner waist diameter because of the maximum evanescent field coupling in the Pd layer. A response time of 30 s was found at 2% with a recovery time of 90 s in Ar. The authors suggested that this response time was mainly driven by the diffusion of the hydrogen atoms into the Pd film. After cycling, the loading time and unloading time became 40 and 100 s. According to the authors, this increase was due to the degradation of the Pd over cycles. In spite of the possible degradation, the response is reproducible.

For nanotapered fibers,[27] a 4-nm Pd film was deposited on the nanotapered waist of an SMF. They used a standard telecommunication optical fiber (Corning SMF-28). The waist diameter was limited to 1300 nm for handling reasons. The length interaction was 2 mm. The source was a laser diode emitting at a wavelength of 1550 nm. The intensity decreased with the increase of the hydrogen concentration in a range from 0.8% to 5.2% H_2 in Ar [Fig. 6(c)]. This change in intensity is opposite to the response reported for the EW sensor (where the decrease in the absorption coefficient of the Pd hydride causes an increase in intensity). The authors did not discuss the increase of the intensity observed.

The design of tapered fiber sensors allows for the decrease of the interaction length. This length is, for instance, only 2 mm for the nanotapered sensor. The authors estimate that this length can be decreased to a few hundreds of micrometers. Nevertheless, tapered optical fibers such as SMTF showed a poor reproducibility due to inaccuracies during the fabrication process.[30] The fabrication of the tapered fiber also made the sensor very fragile.

An optical heterostructure fiber was recently proposed by Luna-Moreno and Monzon-Hernandez[31] to achieve a very robust sensor with a high sensitivity. The heterostructure was made of a 3 to 8-mm length SMF, coated with a 10-nm thick Pd and Pd alloy film, sandwiched between two MMFs. Due to the diameter mismatch of the optical fiber core, the light was guided by the cladding of the SMF. The evanescent

Fig. 6 (a) and (b) Unclad MMF's response;[25] (c) and (d) multimode tapered fiber's (MMTF's) response:[26] (c) time response for a taper diameter of 30 (solid line) and 60 μm (dashed line), and (d) I/I_{H_2} versus H_2 for samples of different taper diameters: 30 (squares), 40 (rhombs), 50 (triangles), and 60 μm (dots);[26] (e) and (f) single-mode tapered fiber's (SMTF's) response; (g) and (h) nanotapered fiber's hydrogen response: time and dynamical ranges.[27]

field was hence strongly coupled in the sensitive layer. The intensity increased upon Pd hydrogenation from 0.8% to 4.6% H_2 in Ar. The relative change in intensity increased with longer interaction length.

Kim et al. presented in 2007 a side-polished SMF as a hydrogen sensor.[32] A jacket-removed SMF was embedded in a quartz fiber holding groove and side-polished. The radius of curvature of the circular groove was 50 cm. After polishing, the cladding thickness left was 2 μm. The interaction length was 2.46 mm. 20-, 100-, and 40-nm Pd films were, respectively, deposited on the side-polished surface by a thermal evaporator. The length of the fiber between the output polarizer and the transducer was only 2 cm in order to minimize the possible polarization entanglement. The hydrogen measurements were performed at 1% and 2% H_2 in Ar at a wavelength of 1550 nm.

The sensor principle is based on the propagation losses of the guided mode. The intensity increased upon Pd hydrogenation for the TM polarization, but the TE response of the sensor was negligible. According to the authors, the TE polarization field cannot penetrate into the metal deeply enough to be affected by the metal film. Consequently, the TE polarization can serve as a reference. Finally, the response and recovery times were 100 and 150 s, respectively.

We conclude the review of EW hydrogen sensors by mentioning the work done by Barmenkov[33] to introduce the measurement of hydrogen concentration into the time domain. The author placed the Pd-tapered fiber as a hydrogen sensing element in a fiber laser cavity based on an Er-doped fiber laser. The attenuation of the sensing element upon hydrogenation decreased the cavity losses, which resulted in decreasing the buildup time. By measuring the changes in the laser buildup time, the author had access to the hydrogen concentrations.

2.4.5 *Surface plasmon hydrogen sensor response*

Surface plasmon resonance (SPR) sensors can be considered as a variety of EW sensors. Because surface plasmon (SP) may propagate at the interface between a Pd thin film and a dielectric medium, the EWs presented above may sometimes be considered as SPR sensors. Strictly speaking, EW is considered as an SPR sensor when the guided light matches with the wavevector of the SP.

In 1998, Bevenot demonstrated an optical fiber hydrogen sensor based on SPR.[16] The sensor consisted of a Pd layer deposited on the MMF core (diameter of 400 μm, NA = 0.48), after removing the optical cladding over a section (2 cm). Note that the design is similar to Tabib-Azar's sensor. The light was injected into the fiber with an appropriate angle of incidence and at a given wavelength (670 nm). The hydrogen concentration was determined by measuring the change in the transmitted intensity of the excited mode groups. The hydrogen response of the sensor depends strongly on the incident angle. From theoretical simulation, an optimal angle of 12 deg was found for 4% H_2.

The measurements were carried out in a hydrogen range of 0.8% to 100%. The intensity increased and changed as a function of H_2 in the same way as the pct of Pd. The response can be related to the two phases α and β, for the concentration ranges of 0.8% to 1% H_2 and 3% to 100% H_2, respectively. Between 1% and 3% H_2, the response strongly varies representing the phase transition. The response time varies

between 3 and 300 s for 100% H_2. Finally, the authors achieved a two-point detection by inserting two sensing zones along an optical fiber.

One argument is to describe that the change is caused by the modification of the SPR due to the variation in the Pd complex permittivity. Although the SPR resonant angle occurs at an angle beyond the fiber NA, the modification is observable due to the presence of a wide SPR peak. As a result, the intensity changes only for the TM polarized light since the SP is only excited for TM polarization.

2.5 *Wavelength-Modulated Hydrogen Sensor Response*

2.5.1 *Fiber Bragg grating sensor*

Sutapun et al.[34] studied the design of a Fiber Bragg grating (FBG) sensor for hydrogen detection in 1999. The sensor was achieved by depositing a 560-nm Pd layer onto the optical cladding of an SMF (5 to 10 μm/125 μm), where an FBG (with Bragg wavelength of 829.73 nm) was previously inscribed. A part of the cladding was etched, and the final cladding had a value of 35 μm.

The expansion of the Pd hydride upon hydrogenation stretched the fiber. The periodicity and the effective index were altered which resulted in shifting the Bragg wavelength. This FBG hydrogen sensor acts as a pure strain sensor. The determination of the Bragg wavelength makes it possible to quantify the H_2 concentration. In this case, the resolution of the spectrometer of 0.14 nm was not adequate to measure the Bragg wavelength shift (less than 0.1 nm). They determined the shift by applying a spline-fitting routine to the data measured (Fig. 7).

The Bragg wavelength increased linearly as a function of H_2 concentration in the range of 0.3% to 1.8% H_2. After exposure to 1.8% H_2, the Pd coating peeled off, which destroyed the sensor. The authors proposed to add a thin adhesion layer to overcome the Pd degradation.

2.5.2 *Grating development*

FBG is insensitive to the surrounding medium refractive index since the resonance results from the core modes coupling. Meltz et al.[37] in 1996 proposed to use FBG written in D-fibers to make the FBG sensitive to the surrounding medium refractive index via EW interactions. In this direction, in 2008, Tien et al.[38] deposited a Pd film on a side-polished fiber over a length of 12 nm (SMF-28, 10 μm/125 μm). A FBG was previously inscribed (grating period of 0.534 μm, length of 20 mm: resonance 1545 nm) in the optical fiber. A 20-nm thick Pd film can be used thanks to the evanescent field interactions. The wavelength resonance shifts to a higher wavelength in the presence of H_2. The shift increased with the increase of H_2 for a range of 20% to 70%. In continuation of this work, Buric et al.[36] studied the response of such a sensor in a range of 1% to 5% H_2 (Fig. 7). They pointed out that the evanescent coupling came from the excitation of the SP at the Pd air interface. Consequently, the sensor was TM polarization dependent. The response time is in the order of a few minutes.

Maier et al.[39] developed, in 2007, a new sensor package to amplify the strain caused by the Pd expansion. The sensor consisted of a semicircular cross-section Pd tube in which a fiber containing an FBG was attached coaxially under
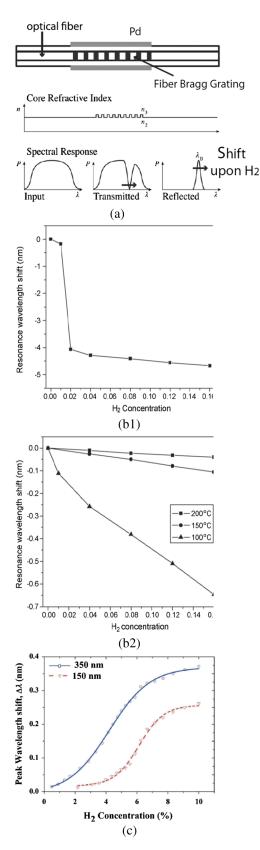
(a)

(b1)

(b2)

(c)

Fig. 7 (a) Schematic of a typical hydrogen sensor based on Pd-coated fiber Bragg grating (FBG); (b) and (c) the response of (b) Wei et al.'s LPG (long-period grating) sensor[35]: (b1) gives the resonance wavelength shift as a function of H2 concentration at 30°C, and (b2) at 100°C, 150°C and 200°C and (c) Buric et al.'s[36] FBG sensor. The sensor responses are described by the sensitivity considered as a function of hydrogen concentration.

tension to a mounting element. Upon hydrogenation, the Pd sensor expanded a half tube. The axial component of this expansion was mechanically collected and redirected into a short section of fiber containing an FBG. A minimal thickness of 300 μm has to be chosen to ensure the stability.

In 2006, Trouillet et al.[40] experimentally replaced the short-period grating (FBG) by an LPG. The device consisted of depositing a 50-nm Pd layer on an SMF (Corning SMF 28) by thermal evaporation after removing the jacket. In contrast to an FBG which uses the fundamental mode propagating through the core, LPG was mainly based on the coupling between the cladding modes and the evanescent or SP at the interface between the Pd coating and the outer medium. Therefore, the sensor was sensitive to the change of the Pd refractive index. The determination of the shift of the loss peaks gave access to the hydrogen concentration [Fig. 7(d)]. At 4% H$_2$, a shift in the order of -5 to -7 nm toward the lower wavelengths was observed in comparison with a shift of 14 pm that was obtained for an FBG (50-nm Pd deposited on fiber with FBG).

In conclusion, depending on the selected OFS, the sensor measures the hydrogen concentration by measuring either the Pd hydride expansion, the Pd refractive index, or the heat release, as described in Table 1.

3 Discussion on H$_2$ Optical Fiber Sensor Performances

3.1 Hydrogen Concentration Range

The performances claimed in the literature for the various sensor technologies are summed up in Table 2 and depicted in Fig. 8.

Phase modulated: The dynamic range of an interferometric hydrogen sensor in this case is limited by the α-phase. For a concentration above the pressure plateau, the Pd layer is deteriorated. Hydrogen interferometric sensors show the highest sensitivity for very low concentrations. The minimal detection is estimated to be a few ppb and is mainly limited by the temperature fluctuations.

Amplitude modulated: The hydrogen OFS based on amplitude modulation shows different dynamic ranges, but the range is generally from 0.5% to 100% H$_2$. Above 3% of H$_2$ in Ar, most of the sensors saturate. The minimal detection is around a value of 0.1% to 0.5% for these sensors, and

Table 1 Operating mechanism of the optical fiber hydrogen sensors.

Modulation		Pd in change		
		Optical	Mechanical	Temperature release
		X	X	X
Phase Polarization Amplitude		No	Negligible	X
		X	Negligible	No
Wavelength	FBG	No	X	
	EW FBG	X	X	
	LPG	X	X	

Note: FBG, fiber Bragg grating; EW, evanescent wave; LPG, long-period grating.

Table 2 Compared performances of existing hydrogen sensors. The sensitivity S defines the change in the signal measured in the presence of H_2, i.e., the fringes shifts, the ratio between the intensity with and without H_2 (I_{H_2}/I_0), the shifts of the resonant wavelengths ($\lambda_{resonanceH_2} - \lambda_{resonance}$) for the phase, amplitude, and wavelength modulations, respectively.

Device	Minimal detection limit	Sensitivity at 4% H_2	[H_2] range %	Pd thickness	Response time at 4% H_2	Resolution (+)
Mach–Zehnder	10^{-4}%		10^{-4}% to 3%	10 μm	3 min	10^{-4}%
Michelson	2×10^{-6}%		2×10^{-6} to 0.1%	500 μm		2×10^{-6}%
Fabry–Perot	3.5×10^{-3}% (predicted)			2 μm		
Bridge configuration	10^{-2}%		10^{-2}% to 0.1%	125 μm	Few days	1.6×10^{-5}
Polarization modulation			1% to 10%	6 nm	1 min (2.8%)	
Micromirror	0.2%	26%	0.2% to 100%	10 nm		
Micromirror	1%	17%	1% to 100%	13 nm	17 s	
SPR	0.8%	26%(****)	0.8% to 100%	12 nm	14 s	
TSMF	1.8%	Close to 50%	1.8–10%	12 nm		
TMMF	0.3%	0.37%	0.3% to 3.5%	15 nm	30 s	
MMF	0.2%	40	0.2% to 0.6%	10 nm	20 s	
Heterostructure	0.8%	0.6%	0.8% to 5%	10 nm		
Nanofiber	0.05% estimated	Close to 35%	0.8% to 5.2%	4 nm	10 s	
FBG	0.2%		0.3% to 1.8%	560 nm		1.95×10^{-2} nm/ 1%H_2 (*)
FBG		14 pm	4%	50 nm	2 min	
FBG	0.5%	0.37 nm (350-nm Pd); 0.26 nm (150-nm Pd)	0.5% to 10%	350 nm 150 nm	30 s(**)	
FBG	125×10^{-4}%	2.8 nm	125×10^{-4}% to 0.1%	300 μm	Few days (at 100 ppm H_2)	0.7 pm/10^{-4}%
LPG		5.7 nm (depends on modes)	4%	50 nm		
LPG	2.7×10^{-2}%	43 pm (1% H_2)	−4%	40 nm	Inferior to 42 s (1% H_2)	
LPG	1%	4 nm	1% to 18%	70 nm	Inferior to 70 s	
LPG	20%		20% to 100%	20 nm		

Note: (+)The resolution is given by the authors. However, since the response is nonlinear, the resolution could also be nonlinear.; (*)Determined in the linear phase.; (**)2 s if the Pd film, I, heated.; (***)We determined a sensitivity of 2% from their sensor responses.; (****)We determined a sensitivity of 10% from their sensor responses.

it is mainly limited by the light fluctuation. A stable light source could decrease this minimum as well as could a reference source. The minimal detection is maximal for the nanotapered fiber sensor. The authors estimated it to be 0.05% H_2. Around 2%, a large change is often obtained: for example, 1.8% to 4.2% and 2% to 3% for SMTF[41] and SPR,[42] respectively. We emphasized that the sensor response amplitude is actually due to the Pd pct, as clearly pointed out in the micromirror section (thin films on substrates). However, there are some discrepancies as described in the following:

- The response saturates are above 0.5%, 2.3%, and 4.2% for the MMF,[25] MMTF,[26] and SMTF,[28,41] respectively.

The saturation of MMF evanescent sensors above 0.5% (Fig. 6b) is probably due to an error in gas mixing. Additional data above 0.6% for this sensor should allow us to comment on this behavior.

- EW and SPR sensors show higher sensitivity when the Pd hydride is in the α-phase or in the β-phase, in comparison with micromirrors systems. The SMTF[41] sensor, for instance, saturates above 4.2%, but a change in the signal is still observable and measurable until 10% H_2.

Wavelength modulated: The dynamic range is analog to the OFS based on amplitude modulation. The response
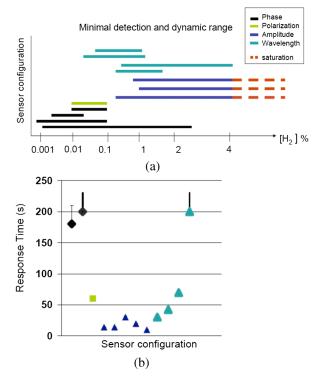
(a)

(b)

Fig. 8 Reported performances of existing hydrogen fiber sensors: (a) gives the minimal detection and dynamic range as a function of sensor configuration, (b) gives the response time as function of the sensor configuration.

reveals the allure of the Pd isotherm. The minimal detection is generally comparable with EW sensors. The best value for the minimal detection for FBG is 125 ppm with the "bridge" design.[39]

We conclude that, in regard to the dynamical range and minimal detection, the H_2 sensitivity of the OFS can be tuned by the appropriate configuration. Nevertheless, the sensor response is limited by the pct of the Pd film used. The level of the slope of the equilibrium pressure plateau as well as the hydrogen solubility are determined by: the microstructure of the Pd (i.e., the deposition condition: deposition pressure, sputtering deposited or evaporated), the Pd thickness, the nature of the substrate (related to the surface energy), and the exterior parameters such as the temperature or the gas environment. There is an intrinsic hysteresis due to the coherent phase transition of the first order. It implies an uncertainty, especially of the plateau pressure, of the pressure read-out. All Pd sensors do not have a limiting cycling lifetime; it depends on the thickness and the clamping layer (e.g., Ti) where the lifetime can be extended.

Therefore, the comparison between the responses may be slightly different since the measurements were carried under different laboratory conditions. The observed difference between the sensors discussed here could actually be due to the morphology of the Pd rather than the sensor itself.

3.2 Response Times of Hydrogen Optical Fiber Sensors at Room Temperature Condition

- Reported responses time at 4% H_2: interferometric and FBG hydrogen OFS based on Pd thick films respond in an order of a few minutes, whereas evanescent and micromirror based on nanometric film respond in an order of a dozen seconds. We conclude that the response time depends strongly on the Pd thickness. As a rule of thumb: the thinner the Pd film is, the faster the response. The fast response (10 s at 4% H_2, room temperature) is obtained for a nanotapered fiber sensor using 3-nm Pd film based on amplitude modulation. In fact, we can distinguish three ranges with some particular cases (see Table 2).

- For a Pd thickness above 1 μm, the response time is in an order of a few minutes.

- For a Pd thickness between 50 and 350 nm, the response time is more than 30 s.

- For a Pd thickness between 10 and 15 nm, the response time varies from 14 to 30 s.

  The observed discrepancy for films having the same thickness is likely due to the experimental conditions such as the deposition conditions, the feed flow, the measurement cell, the room temperature, and the gas environment.

- H_2 concentration dependence: The response time depends on the H_2 concentration. This relation is governed by the rate limited step. The response time is determined by the hydrogen surface adsorption, the surface penetration, the surface dissociation, the bulk diffusion, and the Pd hydride formation.

Kay et al.[43] demonstrated that diffusion is the limiting step for bulk thick film. However, the diffusion is fast enough to reasonably neglect the atomic diffusion for Pd thin film. The diffusion coefficient of the H atoms through the Pd film is $D\alpha = 10^{-7}$ cm^2/s in both the α and β phases. As an example, the response time, predicted by a diffusion limited process, is 40 μs for 20-nm thick α-phase Pd hydride film,[44] which is far inferior to the observed response time. Therefore, the surface dissociation or the diffusion (taking into account the surface penetration and the Pd hydride formation) is the kinetic limited step.

At this time, no consensus was found between scientists. Some works show that the initial absorption rate is linearly proportional to the H_2 pressure, whereas others show a square dependence. The morphology and the quality of the surface could explain the difference observed. In our study, we simply consider that the response time is faster for higher [H_2] than lower [H_2]. Nevertheless, several works reported that the response time is slowed down for hydrogen pressure corresponding to the pressure plateau.[15,44] This phenomenon is attributed to the strain induced by the phase transformation during the expansion of the crystal lattice. Below the phase transition, there is no mechanical change. Above the phase transition, a driven force enhances the absorption although the metal hydride passes by the transition phase. This is due to the difference in thermodynamics.

The recovery of the sensor is always superior to the hydriding time of the sample. The de-hydriding time can be enhanced in an oxygen atmosphere. Oxygen on the surface of Pd will induce the formation of OH and H_2O molecules,[45] which significantly increases the desorption rate.

3.3 Temperature Effects on Optical Fiber Sensor Hydrogen Sensors

Pct dependences: The Pd pcts characterize the phase behavior of metal hydrides. The solubility of an H atom decreases for higher temperatures, and the phase transition disappears for temperatures above the critical temperature. Consequently, at a higher temperature, the sensor response shows a decrease in sensitivity,[16,35,39] but this condition makes H_2 quantification easier due to the apparition of a sloping plateau. For all hydrogen sensors based on metal hydrides, we need to continuously measure/control the ambient temperature in order to calibrate the sensor response.

Sensor dependences: The OFS itself is generally altered in its functions by the temperature. The LPG sensors, for instance, are temperature dependent, and the resonant wavelength shift is significant in comparison with the shift induced by H_2.[39] Wei et al.[35] reported that the change for 4% H_2 in He is smaller than the change induced by 1°C temperature variation for a H_2 FBG sensor.

For achieving an H_2 OFS, the exterior and gas temperature variations have to be measured in order to calibrate the sensor response. A temperature sensor can be added in the hydrogen sensing fiber.

Effect of temperature on OFS response time: The temperature also affects the response time. The kinetics of the hydrogenation is enhanced by increasing the temperature (Arrhenius'relation) and is drastically decreased for lower temperatures. Bevenot et al.[15] proposed to heat the surface by light radiation in order to get an acceptable response time at cryogenic temperatures. The design of the resulting device consisted of a Pd film micromirror deposited at the end of a first optical fiber. The hydrogen concentration is measured by a reflectivity measurement. A second optical fiber is used to heat the Pd surface using light radiation aimed at the entrance of this fiber. Buric et al. recently proposed recently to use FBG to couple the radiated light to the sensitive layer when it is deposited around the core/cladding.

3.4 Cross-Sensitivity in Hydrogen Optical Fiber Sensor Technologies

The performance of the hydrogen sensors described previously and summed up in Table 2 has been validated in an inert environment. For safety applications, the sensor has to operate in air and in presence of other gases for specific applications. Pd is preferably used due to its catalytic properties. In return, other chemical reactions than hydrogenation can occur at the Pd surface. The presence of other gases such as O_2, CO, H_2O, H_2S, and so forth interferes with the absorption of hydrogen. For example:

- Butler and Buss showed that the sensor response time is longer in air than in an inert environment.[14] At low concentration, the response is much slower in air than in N_2. As shown by Petersson et al.,[45] the Pd surface is dominated by adsorbed O below the critical ratio of hydrogen to oxygen partial pressures ($P_{o_2}/P_{o_2} = 0.4$). Similar to oxygen, humidity and CO cause the increase in the response time by blocking the active Pd sites.[46] Note that at elevated temperature (80°C), the cross-sensitivity is reduced.[46]
- The presence of O_2 is also capable of limiting the amount of H_2 absorbed due to the formation of OH

and H_2O on the Pd surface.[47] The change in the sensor signal may be different, resulting in false alarms.

- The presence of H_2S makes the Pd insensitive, which permanently destroys the sensor.

The Pd cross-sensitivity needs to be addressed in order to obtain an efficient and reliable H_2 sensor. However, few studies present the sensor response in oxygen, humidity, or pollutant environments. The cross-sensitivity is mainly a material issue. Regarding the OFS, sensors based on monitoring the surface characteristics such as EW, SPR, and LPG sensors are expected to be the more sensitive to these cross effects.[39] Although oxygen does not penetrate/diffuse in bulk Pd, oxygen is able to penetrate to the interface layer for thin and island films.

There are currently two solutions to circumvent the Pd cross-sensitivity: the use of Pd alloys instead of Pd[45] and/or the use of a protective layer.[47]

The sorption is hampered by adsorbed species. This makes it difficult for hydrogen to find a free Pd site for dissociative adsorption. Pd-based model systems used so far have a limited lifetime and ambiguous read out due to hysteresis and suffer from inhibition by poisonous gases such as CO. To catalyze the hydrogen absorption, we still need to apply a Pd- or Ni-based catalyst, which is easily poisoned. It is obvious that the surface contamination effects play a crucial role when pure hydrogen is used. One solution to increase the H_2 systems' performances is to add a polymer layer on a multilayers configuration. The catalytic properties of Pd alloy thin films are enhanced by a thin sputtered polytretrafluoroethylene (PTFE) coating leading to several improvements in hydrogen adsorption and desorption in Pd-based and Pd-catalyzed hydrogen sensors and hydrogen storage materials.[48] In their paper, Ngene et al.[48] show that the enhanced catalytic performance is attributed to chemical modifications of the catalyst surface by the sputtered PTFE, leading to a possible change in the binding strength of the intermediate species involved in the hydrogen sorption process.

In some applications, PTFE has been used in a Pd-based H_2 sensor as a hydrophobic material to protect Pd from water-based contaminants, but recently, the use of PTFE leads to a significant modification of the catalytic properties of the Pd and Pd-Au surfaces. Clearly, the presence of PTFE leads to a big increase in the hydrogenation kinetics. The authors used a 50-nm $Pd_{80}Au_{20}$ thin film. The addition of a PTFE top layer leads to a visible increase in the loading kinetics and to a profound increase in the unloading kinetics both in pure Ar and in 20% O_2/Ar. The presence of PTFE enhances the recombination of atomic H to H_2 on the Pd-Au surface in that case.

The x-ray analysis shows the presence of carbon implementation into Pd during the PTFE sputter deposition process leading to about a 0.5 eV increase in the binding energy (compared with bulk Pd). Also, the presence of Pd-F bonds is put in relief. The authors suggest that during the PTFE sputtering, some carbon is implanted into the subsurface of the catalyst layer while the Pd-F bonds are mostly formed at the catalyst surface.

One explanation considers the fact that the PTFE is more porous material than the bulk, which explains why H_2, O_2, and H_2O (formed during unloading in O_2 here) are easily transported to and from the catalysts even when coated

with 50-nm sputtered PTFE. Other complementary analysis reveals that the high energy of the Teflon fragments created during the sputter deposition process must have enabled the formation of different Pd-CFx bonds at the surface of the catalyst.

So, the chemical modification results in a more favorable interaction (adsorption/dissociation) of H_2 and O_2 on Pd and Pd-Au surfaces, leading to improved (de)hydrogenation kinetics. For example, the PTFE capped H_2 detectors can be loaded and unloaded more than 40 times in H_2 and O_2 without any noticeable decrease in the kinetics and selectivity of Pd-based catalysts in alkaline hydrogenation and CO oxidation reactions.

One direction of some investigations is to attach some polymer groups on the surface of the Pd nanoparticles (Pd NPs), which led to improved kinetics in the Pd-catalyzed decomposition of formic acid and ambient conditions due to the surface electronic effects. Further investigations can be to improve the kinetics and to tune the selectivity of Pd-based and Pd-catalyzed thin films (de)hydrogenation processes using some other polymer thin films.[48]

4 Conclusion

This analytical review of Pd hydrogen fiber sensors gives an overview of the performances of OFS in hydrogen sensing in terms of sensibility, response time, reliability, reproducibility, and robustness.

In spite of the Pd limitation, Pd is still considered a good material, especially in very thin film form, with which to achieve an effective H_2 sensor.

One direction to investigate this subject can be to study the SPR effect[49–52] and the use of NPs for example.

In this direction, several potential possibilities to design these NPs systems have been and are investigated: pure Pd NP used with different properties (shape) or core shell systems (Pd-Au for example).

The plasmonic effect with some Pd material can be used to achieve some more exotic systems for hydrogen sensing. Tittl et al.[53] reported on the experimental achievement of a Pd-based plasmonic perfect absorber at visible wavelengths. The sensor design is based on Pd nanowires stacked above a gold mirror. The multilayer configuration is an SiO_2 substrate (1 mm)/Au (200 nm)/MgF_2 film (65 nm) and Pd nanowires $(20 \text{ nm} \times 100 \text{ nm})$. The design exhibits a reflectance $<0.5\%$ and zero transmittance at 650 nm. The exposure to hydrogen gas causes a rapid and reversible increase in reflectance on a time scale of seconds.

The continuity to the metal insulator metal systems for detection of hydrogen is to use some thin film materials to get better performances in terms of sensitivity and time response. The use of a polymer layer to protect Pd from water-based contaminants is one solution, but we saw that the use of some polymers can result in an increase in the hydrogenation kinetics.[48]

This effect can also been used in NPs systems using some polymers attached to the Pd NP surface or using NP in a porous polymer layer.

Replacing Pd by Pd alloys seems to be also a relevant approach. The reliability (cross-sensitivity), the reproducibility (lifetime), and the response time will allow the merchantability of the H_2 OFS sensor to be anticipated because the change in the used material will have an important economic impact. Nevertheless, finding a material with high catalytic properties and especially without cross-sensitivity is still one of the "keys" to achieving a fast and reliable hydrogen sensor.

Finally, an appropriate engineering of the pct of metal alloys will permit the tuning of the detection range. In addition, magnesium alloys, such as $Mg_{70}Ti_{30}$, are promising to reach lower minimal detection. In that case, the thin film is stable over ab-desorption cycles and time. The detection layer shows a large optical contrast which drastically decreases the losses in the optical fiber. The response time is strongly dependent on the hydrogen concentration. Mg alloys can be employed with an intrinsic fiber sensor configuration. In contrast to a reproducible Pd film (i.e., around 10 nm), Mg alloys provide a considerably large optical change.[47] In particular, the length of the sensitive layer can be smaller than for Pd-coated sensors (0.5 cm compared with 2 cm). Some other investigations have been done with $Mg_{70}Ti_{30}$ alloys.

References

1. E. Maciak and Z. Opilski, "Transition metal oxides covered Pd film of optical H2 gas detection," *Thin Solid Films* **515**(23), 8351–8355 (2007).
2. M. A. Butler, "Optical fiber hydrogen sensor," *Appl. Phys. Lett.* **45**(10), 1007–1009 (1984).
3. M. A. Butler and D. S. Ginley, "Hydrogen sensing with palladium coated optical fibers," *J. Appl. Phys.* **64**(7), 3706–3712 (1988).
4. W. M. Muller, J. P. Blackledge, and G. G. Libowitz, "Metal hybrides," Technical Report (1968).
5. R. Hugues and J. Jarzynski, "Static pressure sensitivity amplification in interferometric fiber optic hydrophones," *Appl. Opt.* **19**(1), 98–107 (1980).
6. F. Faralhi et al., "Interferometric fibre optic hydrogen sensor," *J. Phys. E* **20**, 432 (1987).
7. D. A. Jackson et al., "Elimination of drift in a single mode optical fiber interferometer using a piezoelectrically stretched coiled fiber," *Appl. Opt.* **19**(17), 2926–2929 (1980).
8. J. S. Zeakes et al., "Modified extrinsic Fabry Perot interferometric hydrogen gas sensor," in *Proc. IEEE Laser in Electro Optics Society Annual Meeting LEOS'94*, Vol. 2, pp. 235–236 (1994).
9. D. Innnuzzi et al., "A fiber-top cantilever for hydrogen detection," *Sens. Actuators B* **121**(2), 706–708 (2007).
10. Y. H. Kim et al., "Hydrogen sensor based on a palladium coated long period fiber grating pair," *J. Opt. Soc. Korea* **12**(4), 221–225 (2008).
11. R. E. Dessy and E. W. Richmond, "Birefringent single arm fiber optic enthalpimeter for catalytic reaction monitoring," *Anal. Chem.* **64**(13), 1379–1382 (1992).
12. M. A. Butler, "Fiber optic sensor for hydrogen concentrations near the explosive limit," *J. Electrochem. Soc.* **138**(9), L46–L47 (1991).
13. M. A. Butler, "Micromirror optical fiber hydrogen sensor," *Sens. Actuators B* **22**(2), 155–163 (1994).
14. M. A. Butler and R. J. Buss, "Kinetics of the micromirror chemical sensor," *Sens. Actuators B* **11**(1–3), 161–166 (1993).
15. X. Bevenot et al., "Hydrogen leak detection using an optical fibre sensor for aerospace applications," *Sens. Actuators B* **67**(1–2), 57–67 (2000).
16. X. Bevenot, "Etude de la faisabilité et réalisation d'un capteurd'-hydrogène à fibresoptiques pour des applications aérospatiales," PhD Thesis, Université Jean Monet de Saint Etienne (1998).
17. A. Armgarth and C. Nylander, "Blister formation in Pd gate mis hydrogen sensors," *IEEE Electron Device Lett.* **3**(12), 384–386 (1982).
18. R. F. A. Gremaud, "Hydrogenography: a thin film optical combinatorial study of hydrogen storage materials," PhD Thesis, Vrijeuniversiteit (2008).
19. A. A. Kazemi et al., "Fiber optic hydrogen sensor leak detection system for launch vehicle applications," *Proc. SPIE* **6379**, 63790D (2006).

20. J. A. Garcia and A. Mandelis, "Study of the thin film palladium/hydrogen system by an optical transmittance method," *Rev. Sci. Instrum.* **67**(11), 3981–3983 (1996).
21. K. Kalli, A. Othonos, and C. Christofides, "Characterization of reflectivity inversion, α- and β-phase transitions and nanostructure formation in hydrogen activated thin Pd films on silicon based substrates," *J. Appl. Phys.* **91**, 3829 (2002).
22. R. J. Matelon et al., "Substrate effect on the optical response of thin palladium films exposed to hydrogen gas," *Thin Solid Films* **516**(21), 7797–7801 (2008).
23. A. Borgschulte et al., "High-throughput concept for tailoring switchable mirrors," *Appl. Surf. Sci.* **253**(3), 1417–1423 (2006).
24. B. Dam et al., "Combinatorial thin film methods for the search of new lightweight metal hybrides," *Scr. Mater.* **56**(10), 853–858 (2007).
25. M. Tabib-Azar et al., "Highly sensitive hydrogen sensors using palladium coated fiber optics with exposed cores and evanescent field interactions," *Sens. Actuators B* **56**(1–2), 158–163 (1999).
26. J. Villatoro et al., "Optical fiber hydrogen sensor for concentrations below the lower explosive limit," *Sens. Actuators B* **110**(1), 23–27 (2005).
27. J. Villatoro and D. Monzon-Hernandez, "Fast detection of hydrogen with nano fiber tapers coated with ultra thin palladium layers," *Opt. Express* **13**(13), 5087–5092 (2005).
28. J. Villatoro et al., "Highly sensitive optical hydrogen sensor using circular Pd coated single mode tapered fibre," *Electron. Lett.* **37**(16), 1011–1012 (2001).
29. J. Villatoro et al., "In line highly sensitive hydrogen sensor based on palladium coated single mode tapered fibers," *IEEE Sens. J.* **3**(4), 533–537 (2003).
30. D. Zalvidea et al., "Wavelength multiplexed hydrogen sensor based on palladium coated fiber taper and Bragg grating," *Electron. Lett.* **40**(5), 301–302 (2004).
31. D. Luna-Moreno and D. Monzon-Hernandez, "Effect of the Pd-Au thin film thickness uniformity on the performance of an optical fiber hydrogen sensor," *Appl. Surf. Sci.* **253**(21), 8615–8619 (2007).
32. K. T. Kim et al., "Hydrogen sensor based on palladium coated side polished single mode fiber," *IEEE Sens. J.* **7**(12), 1767–1771 (2007).
33. Y. O. Barmenkov, "Time domain fiber laser hydrogen sensor," *Opt. Lett.* **29**(21), 2461–2463 (2004).
34. B. Sutapun, M. Tabib-Azar, and A. Kazemi, "Pd-coated elastooptic fiber Bragg grating sensors for multiplexed hydrogen sensing," *Sens. Actuators B* **60**(1), 27–34 (1999).
35. X. T. Wei et al., "Nano-structured Pd-long period fiber gratings integrated optical sensor for hydrogen detection," *Sens. Actuators B* **134**(2), 687–693 (2008).
36. M. Buric et al., "Multiplexable low temperature of uniform waist single mode tapered optical fiber sensors," *IEEE Photonics Lett.* **21**(21), 1594–1596 (2009).
37. G. Meltz, S. J. Hewlett, and J. D. Love, "Fiber grating evanescent wave sensors," *Proc. SPIE* **2836**, 342–350 (1996).
38. C. L. Tien et al., "Hydrogen sensor based on side-polished fiber Bragg gratings coated with thin palladium film," *Thin Solid Films* **516**(16), 5360–5363 (2008).
39. R. R. J. Maier et al., "Fibre optics in palladium-based hydrogen sensing," *J. Opt. A* **9**(6), S45–S59 (2007).
40. A. Trouillet, E. Marin, and C. Veillas, "Fibre gratings for hydrogen sensing," *Meas. Sci. Technol.* **17**(5), 1124–1128 (2006).
41. J. Villatoro, D. Monzon-Hernandez, and E. Mejia, "Fabrication and modeling of uniform waist single mode tapered optical fiber sensors," *Appl. Opt.* **42**(13), 2278–2283 (2003).
42. X. Bevenot et al., "Surface plasmon resonance hydrogen sensor using an optical fibre," *Meas. Sci. Technol.* **13**, 118–124 (2002).
43. B. D. Kay, C. H. F. Peden, and D. W. Goodman, "Kinetics of hydrogen absorption by Pd," *Phys. Rev. B* **34**(2), 817 (1986).
44. Z. Zhao et al., "All optical hydrogen sensing materials based on tailored palladium alloy thin films," *Anal. Chem.* **76**(21), 6321–6326 (2004).
45. L. G. Petersson, H. M. Dannetun, and I. Lundstrom, "Hydrogen detection during catalytic surface evidence for activated lateral hydrogen mobility in the water-forming reaction on Pd," *Phys. Rev. Lett.* **52**, 2 (1984).
46. Z. Zhao et al., "All-optical hydrogen sensor based on a high alloy content palladium thin film," *Sens. Actuators B* **113**(1), 532–538 (2006).
47. M. Slaman et al., "Optimization of Mg-based fiber optic hydrogen detectors by alloying the catalyst," *Int. J. Hydrogen Energy* **33**(3), 1084–1089 (2008).
48. P. Ngene et al., "Polymer-induced surface modifications of Pd-based thin films leading to improved kinetics in hydrogen sensing and energy storage applications," *Angew. Chem.* **53**, 12081–12085 (2014).
49. C. Perrotton, "Design and development of a fiber optic hydrogen sensor," Thesis, University of Strasbourg (2012).
50. C. Perrotton et al., "A fiber optic surface plasmon resonance sensor based on wavelength modulation for hydrogen sensing," *Opt. Express* **19**(S6), A1175–A1183 (2011).
51. C. Perrotton et al., "Wavelength response of a surface plasmon resonance palladium coated optic fiber," *Opt. Eng.* **50**(1), 014403 (2011).
52. C. Perrotton et al., "A reliable, sensitive and fast optical fiber hydrogen sensor based on surface plasmon resonance," *Opt. Express* **21**(1), 382–390 (2013).
53. A. Tittl et al., "Palladium-based plasmonic perfect absorber in the visible wavelength range and its application to hydrogen sensing," *NanoLett.* **11**, 4366–4369 (2011).

Nicolas Javahiraly is an associate professor in physics at the University of Strasbourg, France. He completed a PhD degree in photonics on fiber optic sensors. After a postdoc at Harvard University on interactions between ultrashort laser pulses and matter, he worked as an expert and project manager in Sagem Defense group in Paris. He is now working on nano-optic sensors, nanotechnology, plasmonics, metamaterials, and interaction of laser matter.